Adapted cabling of an EEG cap improves simultaneous measurement of EEG and fMRI at 7T

Meyer, M.C.; Scheeringa, R.; Webb, A.G.; Petridou, N.; Kraff, O.; Norris, D.G.

Journal of Neuroscience Methods 331 (2020) 108518

Contents lists available at ScienceDirect

Journal of Neuroscience Methods

journal homepage: www.elsevier.com/locate/jneumeth

Adapted cabling of an EEG cap improves simultaneous measurement of EEG and fMRI at 7T

Matthias C. Meyer[a,1], René Scheeringa[a,d,*,1], Andrew G. Webb[b], Natalia Petridou[c], Oliver Kraff[d], David G. Norris[a,d]

[a] Donders Institute for Brain, Cognition, and Behaviour, Radboud University Nijmegen, Nijmegen, the Netherlands
[b] C.J. Gorter Center for High Field MRI, Department of Radiology, Leiden University Medical Center, Leiden, the Netherlands
[c] Radiology, Imaging Division, Center for Image Sciences, University Medical Center Utrecht, Utrecht, the Netherlands
[d] Erwin L. Hahn Institute for MRI, University Duisburg-Essen, Essen, Germany

ARTICLE INFO

Keywords:
EEG
fMRI
7T
EEG cap
ERP
Oscillations

ABSTRACT

Background: The combination of EEG and ultra-high-field (7 T and above) fMRI holds the promise to relate electrophysiology and hemodynamics with greater signal to noise level and at higher spatial resolutions than conventional field strengths. Technical and safety restrictions have so far resulted in compromises in terms of MRI coil selection, resulting in reduced, signal quality, spatial coverage and resolution in EEG-fMRI studies at 7 T.

New method: We adapted a 64-channel MRI-compatible EEG cap so that it could be used with a closed 32-channel MRI head coil thus avoiding several of these compromises. We compare functional and anatomical as well as the EEG quality recorded with this adapted setup with those recorded with a setup that uses an open-ended 8-channel head-coil.

Results: Our set-up with the adapted EEG cap inside the closed 32 channel coil resulted in the recording of good quality EEG and (f)MRI data. Both functional and anatomical MRI images show no major effects of the adapted EEG cap on MR signal quality. We demonstrate the ability to compute ERPs and changes in alpha and gamma oscillations from the recorded EEG data.

Comparison with existing methods: Compared to MRI recordings with an 8-channel open-ended head-coil, the loss in signal quality of the MRI images related to the adapted EEG cap is considerably reduced.

Conclusions: The adaptation of the EEG cap permits the simultaneous recording of good quality whole brain (f) MRI data using a 32 channel receiver coil, while maintaining the quality of the EEG data.

1. Introduction

Simultaneous EEG-fMRI allows us to directly relate electrophysiological EEG features to region-specific hemodynamic changes in humans (Debener et al., 2006). Research using this technique has helped us to understand how EEG features, such as: event related potentials and task related power changes, relate to fMRI measures (Debener et al., 2005; Eichele et al., 2005; Ostwald et al., 2010; Porcaro et al., 2010; Scheeringa et al., 2009); the relation between resting state networks and EEG (Mantini et al., 2007; Moosmann et al., 2009; Sadaghiani et al., 2010; Scheeringa et al., 2008, 2012); and the neural underpinnings of the BOLD signal (Scheeringa et al., 2011a, 2016). Furthermore, this technique is often used in epilepsy research and can potentially also provide valuable information for other clinical purposes (Vitali et al., 2015).

Previous studies using simultaneous EEG and fMRI have primarily been carried out at 1.5 or 3 T MRI scanners. In recent years however, high field (e.g. 7 T) fMRI has become a prominent tool for neuroscientists (Balchandani and Naidich, 2015). Among the advantages of measuring fMRI at high field strength are stronger BOLD responses, better intrinsic spatial resolution, and the ability to measure at sub-millimeter resolution over large parts of the brain. Combination of high-field fMRI with simultaneously recorded EEG would open up new possibilities for exploring the relationship between BOLD activation in fine structures (e.g. cortical layers) and electrophysiological features.

Several studies have investigated technical and safety aspects of

* Corresponding author at: Donders Institute for Brain, Cognition, and Behaviour, Radboud University Nijmegen, Nijmegen, the Netherlands.
E-mail address: rene.scheeringa@donders.ru.nl (R. Scheeringa).
[1] Contributed equally

https://doi.org/10.1016/j.jneumeth.2019.108518
Received 22 October 2018; Received in revised form 11 November 2019; Accepted 11 November 2019
Available online 14 November 2019

measuring EEG at 7 T (Abbasi et al., 2015; Brookes et al., 2009; Jorge et al., 2015; Mullinger et al., 2008a, b; Neuner et al., 2013; Poulsen et al., 2017; Vasios et al., 2006). Of these studies, only a few have demonstrated EEG recording during fMRI acquisition at 7 T (Brookes et al., 2009; Jorge et al., 2015; Mullinger et al., 2008a, b; Vasios et al., 2006) as well as a few studies characterizing the EEG signal at high magnetic field strength, but without simultaneously acquiring MR data per se (Abbasi et al., 2015; Neuner et al., 2013). This is partly due to the distortion caused by the EEG equipment, which is more severe at 7 T compared to 3 T (Jorge et al., 2015; Mullinger et al., 2008b; Vasios et al., 2006). A recent study by Jorge et al. (2015) demonstrated that EEG can be safely measured in the 7 T environment with an adapted EEG cap. They demonstrated that their setup allowed for EEG recordings that reliably measured alpha power modulations during an eyes-open/eyes-closed paradigm and visual evoked potentials (VEP) during a reversing checkerboard paradigm. Anatomical MRI and fMRI images were acquired with an open ended 8-channel transmit/receive head loop array (RAPID Biomedical GmbH, Rimpar, Germany). Although good quality fMRI data were recorded from the regions of interest in the visual system, this set-up resulted in reduced signal recorded from dorsal regions in the cortex located close to the open end of the 8-channel coil.

In the set-up described in the study presented here, we adapted an MRI compatible 64 channel EEG-electrode cap to be compatible with a combined 32 channel receive and circularly polarized (CP) birdcage transmit head coil (Nova Medical, Wilmington, MA, USA) which is a cross-vendor distributed RF head coil available at almost every 7 T site. We compared anatomical and functional MR image quality recorded with this coil with that recorded with the aforementioned 8-channel coil, which is the configuration recommended by the EEG manufacturer. We did this for two different 7 T MRI systems from two different vendors (Siemens and Phillips).

During fMRI acquisition, simultaneous EEG was recorded during three different paradigms. In a similar way to Jorge et al. (2015) we assessed alpha power modulation through an eyes-open/eyes-closed paradigm. In our study VEPs were measured in a paradigm that consisted of short presentations of a single checkered wedge in the left inferior visual field, which should lead to activation in the right hemisphere of visual cortex that can be measured with both fMRI and event related potentials (ERP) computed from simultaneously recorded EEG (Scheeringa et al., 2011b). In addition to these two EEG features, we assessed the ability to measure high gamma band activity with this set-up, in a visual attention task in which subjects had to detect a speed increase in the inward contraction of circular gratings presented centrally in the visual field. This paradigm reliably modulates gamma band activity in MEG and EEG measurements (Hoogenboom et al., 2006; Scheeringa et al., 2011a). Together, these three paradigms demonstrate the feasibility to measure evoked potentials as well as (task related) changes in low (alpha) and high (gamma) frequency oscillatory power.

2. Methods

2.1. Subjects

In this study we show data from seven healthy subjects (*age 22–36 years, 1 female*) who participated in this study. In line with the declaration of Helsinki these subjects gave written informed consent. The experiments and measurements with the modified EEG cap at the Erwin L. Hahn Institute were performed under the general ethical approval for conducting MRI research approved by local ethics committees in Essen (Ethics committee of the medical faculty of the University of Duisburg-Essen; Approval number: 11-4898-BO). The modifications of the EEG cap were discussed and approved by the local MR-safety officer. The measurement in Utrecht were carried out under the development protocol (protocol number 15-466) that was approved by the Medical Ethics Committee of the University Medical Center Utrecht. This development protocol enables the use of non-standard or modified equipment in the MRI scanner. The measurement in Leiden was approved by the Medical Ethics Commission of the Leiden University Medical Centre (approval number: 07.096) that included the use of adapted and non-standard equipment in the MRI scanner. A separate measurement in the EEG laboratory at the Donders Institute was carried out under the general ethical approval for EEG-experiments in Nijmegen (approval number: CMO 2014/288; Commissie Mensgebonden Onderzoek, region of Arnhem/Nijmegen).

Four subjects performed all three paradigms at the 7 T Siemens system in Essen, the fourth subject performed two extra sessions of the visual attention paradigm. A fifth subject was measured in a shielded EEG lab in Nijmegen to ensure the subject had a gamma band EEG-response, and subsequently at the 7 T scanner in Essen using the 8-channel receive RAPID head coil (functional images only) as well as the 32-channel receive NOVA head coil (anatomical and functional images). For each coil configuration, this subject performed three runs of the visual attention task. A sixth subject was measured at the 7 T Philips system in Utrecht, performing the visual attention ('gamma') and the eyes open eyes closed paradigms. Furthermore, a T1 image of a seventh subject with fully applied EEG cap (with gel, connected to the amplifiers) was acquired at the 7 T Philips system in Leiden. We compared the quality of the anatomical image and EEG data for the visual attention task of these subjects with the same measures obtained from an eighth subject with an original unchanged cap inside the RAPID coil. For this eight subject the functional data measured simultaneously with the EEG data were measured with a 3D FLASH, sequence, which cannot directly be compared to the 3D EPI sequence used for the other subjects and is therefore not shown here. The experiments performed are summarized in Table 1.

2.2. The modified EEG cap

The 32-channel NOVA head receive coil has a closed soccer ball design split in two parts: an anterior and posterior receive array, surrounded by a birdcage coil for RF transmission (see Fig. 1 B) and C)). When placing a subject inside the NOVA coil, the transmit coil and the anterior part of the receive array can be moved to the back, so that the head of the subject can easily rest on the posterior part of the receive coil. Once the subject lies at rest, the anterior part of the receive coil and the transmit coil can be pushed back to close the coil. When open, there is a small opening at the back of the coil between the two coil halves and in a closed state there remains a small gap between the anterior and posterior parts of the receive coil. To modify the MR-

Table 1
Overview subjects and measurements.

Subject	place / manufacturer	Coil	T1 scan	VEP	Eyes open/ closed	Gamma
S1	Essen/Siemens	RAPID				
		NOVA	x	1	1	1
S2	Essen/Siemens	RAPID				
		NOVA	x	1	1	1
S3	Essen/Siemens	RAPID				
		NOVA	x	1	1	1
S4	Essen/Siemens	RAPID				
		NOVA	x	1	1	3
S5*	Essen/Siemens	RAPID				3
		NOVA	x			3
S6	Utrecht/Phillips	RAPID				
		NOVA	x	1	1	
S7	Leiden/Phillips	RAPID				
		NOVA	x			
S8	Essen/Siemens	RAPID	x			3
		NOVA				

Numbers indicate the number of blocks per task. * Three blocks of the gamma task were recorded earlier in the EEG lab.

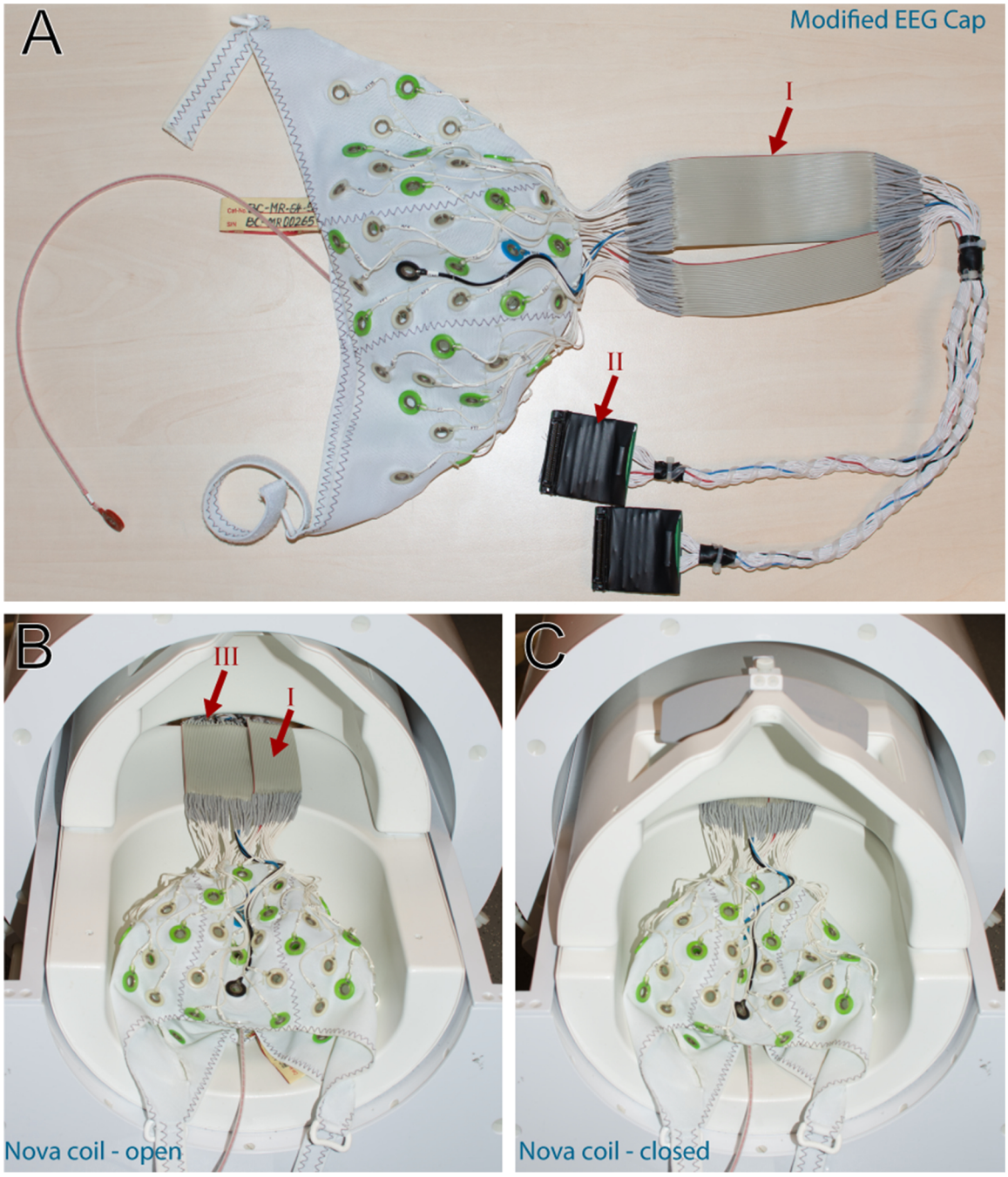

Fig. 1. The cable of the adapted 64 channel EEG cap is designed to fit the NOVA head coil. Indicated by the arrows are the adapted flattened cable (A) and connectors (B) and the small gap between the two halves of the NOVA coil through which the flattened cable is led (C).

compatible 64-channel EEG-Cap (Easycap, Brain Products, Gilching, Germany) to be compatible with the NOVA head coil, the cable and connectors had to be customized in a way to fit through the small opening at the back of the NOVA coil when it is open, and still allow the coil to close. Therefore, the casing of the connectors was removed, the solder points on the connector circuit board were filed off and the board was wrapped with insulating tape. The cable of the EEG cap was cut and a flat cable was soldered between the cap part and the connector part of the cable (See Fig. 1 A). The length of the flat cable part (14.5 cm) was chosen to be long enough to fit the NOVA coil but as short as possible to reduce EEG artifacts. Furthermore, in order to reduce MR artifacts, cable bundle lengths were minimized when connecting the electrode cables from the EEG cap to the flat cable. The solder joints at both ends of the flat cable were covered by heat shrinkable tubing.

2.3. Safety concerns

In order to test the new setup a dummy scan was performed on a spherical oil phantom (Siemens Healthcare, Erlangen, Germany) to examine whether the new EEG cap interferes with the NOVA head coil. B1 maps were acquired using the 2D DREAM sequence (Nehrke and Bornert, 2012) to examine B1 distortions. Since the EEG cap has been labeled MR conditional at 7 T in combination with the Rapid coil by the vendor, and after studying the safety-related numerical simulations published by Jorge et al. (Jorge et al., 2015), it was agreed to not perform extensive numerical simulations with a model of the Nova head coil, but to limit the specific absorption rate (SAR) to 50 % or less of the maximum allowed value for normal operating mode.

Prior to the scans, all subjects were instructed to immediately report

any sensation of heat or discomfort. Additionally, the body temperature of each subject was monitored before and after the scan session using an in-ear thermometer. Only healthy volunteers with no known history of diabetes or cardiovascular disease that could impair the subjects' thermoregulation were imaged.

2.4. Experimental paradigms

To determine the data quality from the new EEG cap, three distinct paradigms were used in order to cover a broad range of applications. One paradigm ("VEP paradigm") was designed to generate visual evoked potentials (VEPs) by presenting a high contrast visual stimulus. The second paradigm ("Alpha paradigm") was designed to alter the power in the alpha EEG frequency band, by opening and closing the eyes. The third paradigm ("Gamma paradigm") was a visual attention task that is known to elicit strong, long-lasting (up to several seconds), and narrow-band gamma activity in MEG (Hoogenboom et al., 2006; Muthukumaraswamy and Singh, 2008) and EEG (Koch et al., 2009; Scheeringa et al., 2011a). The paradigms are described in more detail below.

2.4.1. VEP paradigm

Fig. 2A schematically depicts the design of the simple visual VEP paradigm. The subjects were asked to lie relaxed in the scanner and to always focus on a central fixation cross. Each subject performed 20 min. blocks in which 10 stimuli (750 ms presentations of a lower left-quarter checkerboard wedge with 100 % contrast) were presented with a randomized inter-stimulus interval of 2–2.5 s. After each mini-block there was a 15 s pause during which a fixation cross was presented.

2.4.2. Alpha paradigm

The subjects were asked to lie relaxed in the scanner and to look at a central fixation cross with eyes open. Red and white flickering text with contrasting red and white background was presented to inform the subject to open or close their eyes. These stimuli were bright enough to be easily recognized with closed eyes.

Ten blocks of 20 s eyes open and ten blocks of 20 s with eyes closed were presented.

2.4.3. Gamma paradigm

Subjects performed the visual attention task shown in Fig. 2B. In order to obtain a sufficient signal-to-noise ratio (SNR) in the EEG gamma frequency band, an interleaved MR sequence was used where trials were presented in breaks between the acquisition of three MR volumes. In this task, subjects attended to circular, inward moving gratings, and were asked to detect a change in inward speed.

Each trial started with a reduction in contrast of a fixation point that was presented between trials (Gaussian of 0.4 ° width) by 40 %. This contrast reduction served as a warning for the upcoming visual stimulation, and instructed the subjects to stop blinking until the end of the trial. After 1600 ms, a red '!' or a green '=' appeared just above the fixation point for 100 ms. The '!' indicated a 66.7 % chance of an increase in the speed of the upcoming inward moving grating and was presented in 75 % of the trials. The '=' indicated that no speed change would occur and was presented in 25 % of the trials. After this attention cue was removed, the fixation point remained on the screen for 400 ms before it was replaced by a sine wave grating (diameter: 7°; spatial frequency: 2.5 cycles/degree; contrast: 50 %). The sine wave grating contracted to the fixation point (1.6 degrees/sec) for one of three stimulus durations: 1200 (25 % of the trials), 1400 (25 %) or 1600 ms (50 %). This was followed by an increase in the contraction speed to 2.2 degrees/sec for maximally 500 ms after either 1200 or 1400 ms. Trials with 1600 ms stimulation were not followed by a speed change. Therefore, trials cued with '=' were always followed by a 1600 ms visual stimulation period, while for trial trials cued with '!' this happened in 33.3 % of the trials. An equal number of trials of the four conditions were presented (1200 ms stimulation, attended, speed change; 1400 ms stimulation, attended, speed change; 1600 ms stimulation, attended, no speed change; 1600 ms stimulation, not attended, no speed change).

Subjects were instructed to press a button with their right index finger as soon as they detected the speed change. The stimulus disappeared after a response was given, after 1600 ms of stimulation (for catch trials), or if no response was given within 500 ms after the speed change. Feedback about the performance was given for 500 ms. In the case of a correct response or if a response was correctly withheld, 'ok!' appeared in green above the fixation point. In case of premature or slow/no responses, 'early' or 'late' respectively appeared in red.

Each block consisted of 72 trials, 18 for each condition. The onset of a trial was triggered every third MRI volume. The MRI sequence we used consisted of the acquisition of three volumes each of 4.128 s (for experimental details see below) followed by a scan-free period of the same length to allow for MR gradient- and RF pulse-free recording of EEG data during the presentation of the trial. The trial, starting with the

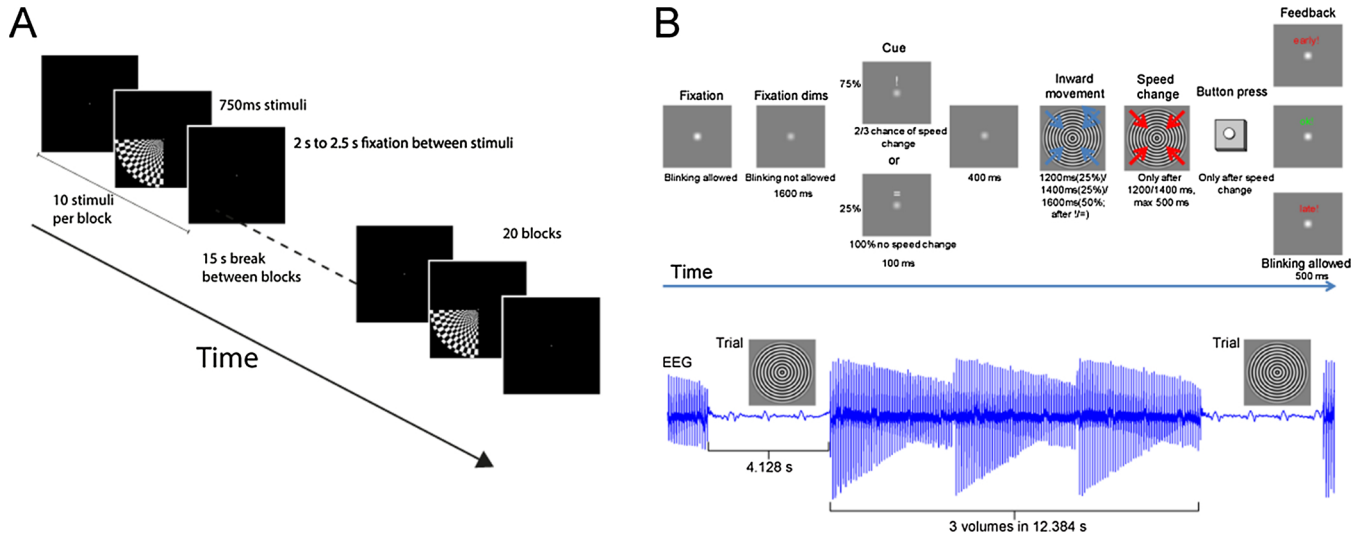

Fig. 2. Schematic depiction of the VEP paradigm (A) and gamma (B) paradigms.
Since residual gradient artifacts would hinder the observation of the relative small gamma response, the trials were presented during pauses in the fMRI sequence, as indicated in the lower part of (B).

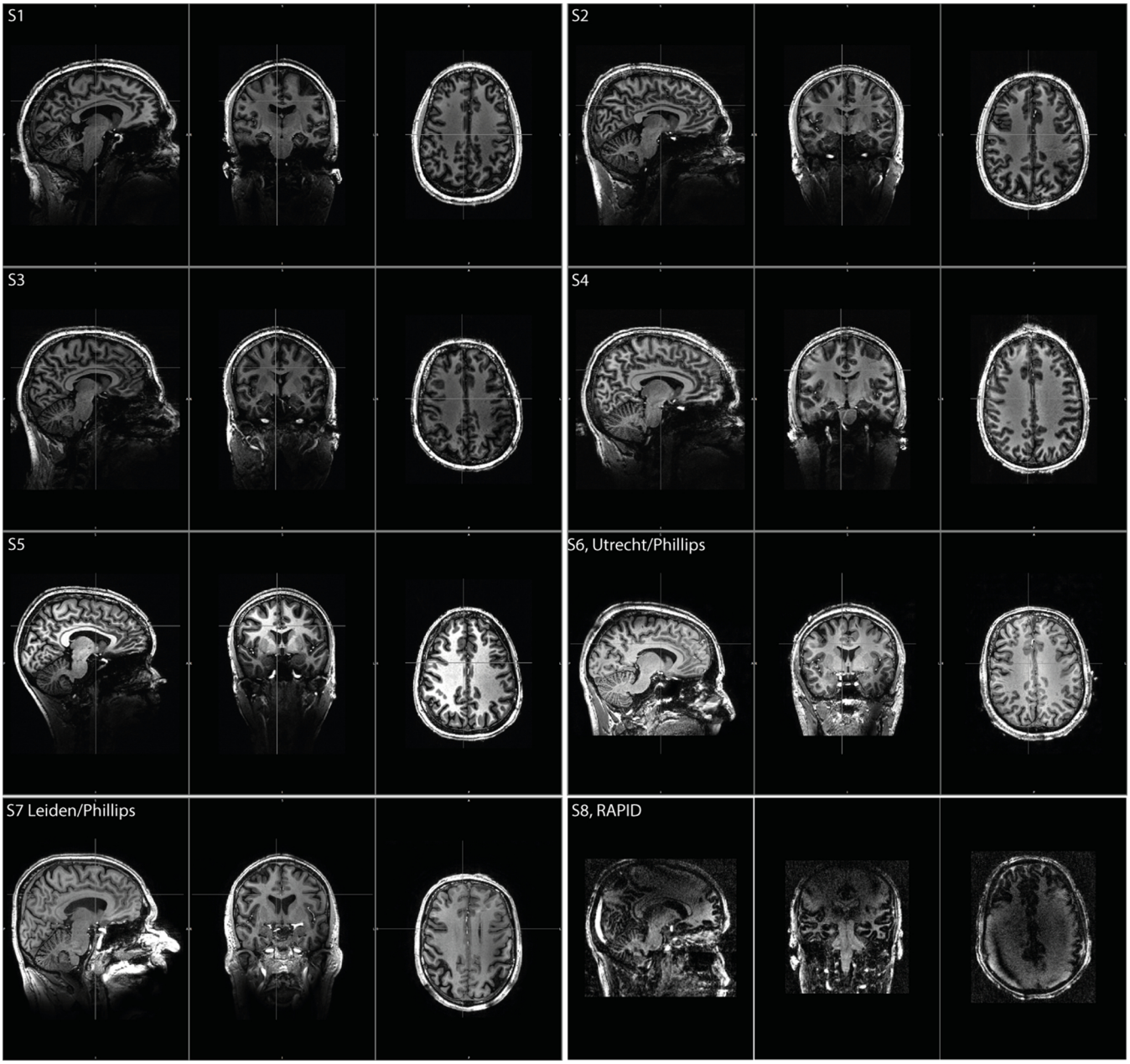

Fig. 3. Anatomical scans with EEG cap applied. Note that the recommended setup, with a common 64 channel EEG cap and the RAPID coil (S8, RAPID) leads to severe signal dropout at the upper part of the head. In the other panels the anatomical scan was obtained using the new 64 channel EEG cap with the NOVA head coil. This setup significantly improves the image quality of the T1 images which are reproducible across subjects, sites and systems.

dimming of the fixation point, commenced 340 ms after the end of the acquisition of the third scan within the 4.128 s gap. The attention cue was presented in the artifact free period, without switched magnetic gradients or RF pulses, 1260 ms after the end of the third scan; the stimulation onset was at 1760 ms. A trial was presented every 16.512 s (see Fig. 2). In total each session was 19 min and 49 s long.

2.5. (f)MRI data acquisition

2.5.1. Essen

MRI measurements were performed on a 7 T whole-body MR system (Magnetom 7 T, Siemens Healthcare GmbH, Erlangen, Germany) with a 32 channel head coil (NOVA Medical, Wilmington, USA). Functional images were acquired using a 3D gradient echo planar imaging (EPI) sequence (Poser et al. 2010) (volume TR = 4128 ms, TE = 30 ms, flip angle = 17 degrees, 0.9 mm isotropic voxels using a 220 mm FOV with a 240 × 240 matrix and 64 slices with 0.9 mm thickness, GRAPPA 4 acceleration). To improve EEG data quality during the gamma paradigm, the 3D EPI sequence was modified to allow a delay after every third volume. Thus, after three MR volumes were acquired, a pause of 4128 ms occurred, during which time the gamma paradigm was presented. For the functional measurements with the RAPID coil we also used a 3D gradient echo EPI sequence (volume TR = 3792 ms, TE = 28 ms, flip angle = 17 degrees, 0.8 mm isotropic voxels using a 192 × 190 mm FOV with a 240*238 matrix and 48 slices with 0.8 mm thickness, GRAPPA 4 acceleration).

A 3D MP2RAGE sequence (Marques et al. 2010) was used to acquire the anatomical T1 scan (inversion times 800 ms and 2700 ms with flip angles of 4 and 5 degrees, TR = 6000 ms, TE = 3.06 ms, 0.75 mm isotropic voxels using a 240 mm FOV with a 320 × 320 matrix and 224 slices with a 50 % slice gap, GRAPPA 3 acceleration, phase and slice partial Fourier factors of 6/8, bandwidth 240 Hz/pixel). Gradient

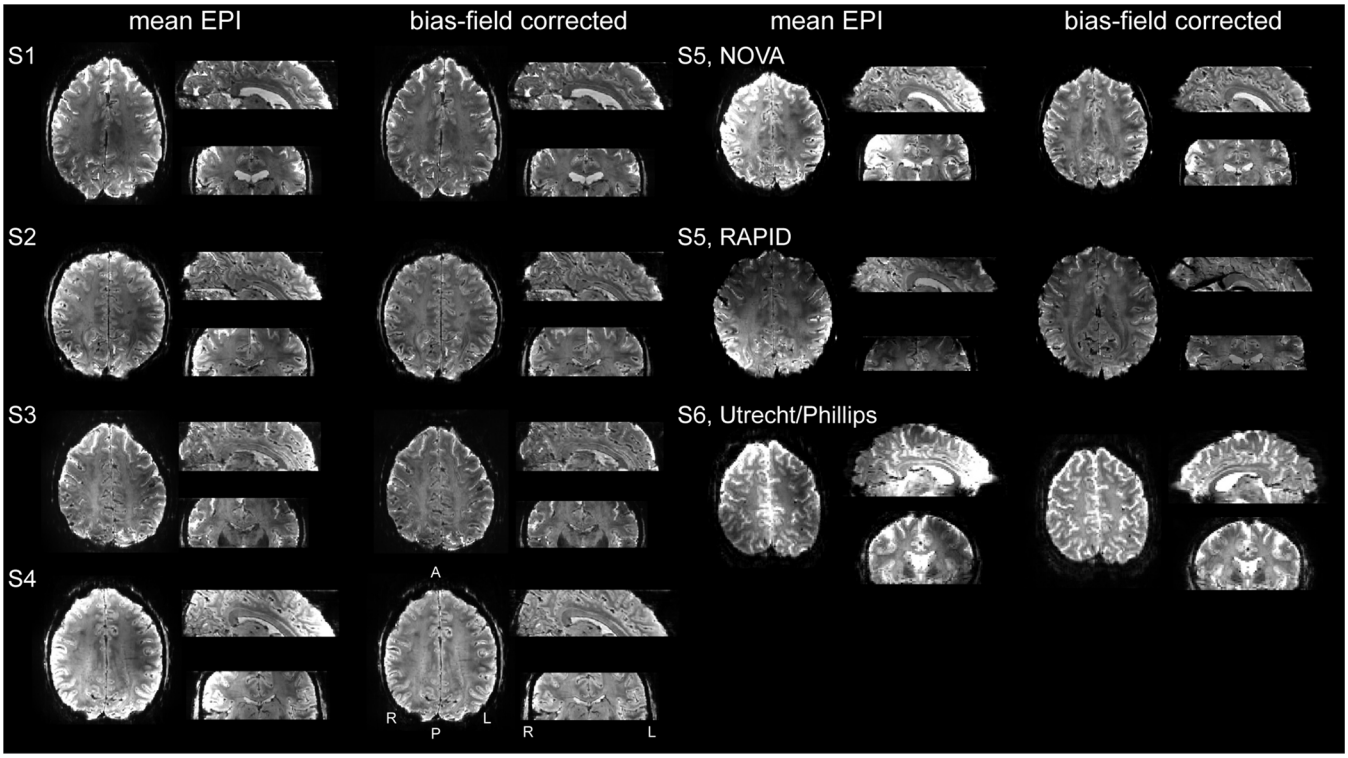

Fig. 4. Mean functional EPI scans before and after bias field correction measured with the adapted EEG cap applied. For all subjects, except subject 5, the mean EPI after motion correction is depicted for the VEP task. For subject 5, the mean functional scan for the gamma task was used. For this subject the mean functional image recorded with both NOVA and RAPID coils are depicted.

echo (GRE) field maps were acquired to aid in B0 distortion correction, and B1 maps were acquired using the 2D DREAM sequence to monitor B1 distortions caused by the EEG cap. The MR system`s helium cold heads were switched off during all EEG measurements to minimize vibrations affecting EEG data quality (Mullinger et al., 2008a).

2.5.2. Utrecht and Leiden

MR data in both Utrecht and Leiden were acquired on a 7 T Philips Achieva system (Philips, Best, the Netherlands). In Utrecht, functional images were acquired with a single-shot multi-slice EPI sequence with the following parameters: TR: 3 s, TE: 25 ms, flip angle: 80 degrees, 1.8 mm isotropic voxel size, FOV: 222 × 186 × 90 mm^3 (AP x RL x IS), 50 axial slices with no gap, SENSE acceleration factor 3 (AP direction). FMRI data were acquired for the VEP paradigm (300 repetitions, scan duration 15 min, 1 run) and for the alpha (eyes open/eyes closed) paradigm (220 repetitions, scan duration 11 min, 1 run). Anatomical T1-weighted images were acquired with a three dimensional T1-weighted gradient-echo sequence with the following parameters: TR/TE = 7 / 2.86 ms, flip angle = 8 degrees, adiabatic inversion with inversion time (TI) 1100 ms, FOV: 252 × 190 × 200 (AP x RL x IS), 0.8 mm isotropic voxel size, 238 sagittal slices, SENSE factor = 1.8 × 1.8 (AP x RL).

In Leiden, the anatomical image was acquired using a three dimensional T1-weighted gradient-echo sequence: FOV: 220 × 224 × 200 mm, spatial resolution 1 × 1 × 1 mm^3, adiabatic inversion pre-pulse, TR/TE/TI/flip angle = 4.3 ms/1.93 ms /1300 ms/7°, SENSE factor 2.9 in R/L direction.

2.6. EEG recording

At all 7 T sites, the EEG data were recorded from 64 scalp positions, according to the international 10−10 system, using the modified 64-channel EEG cap. Signals were recorded with two 32-channel MRI-compatible EEG amplifiers (BrainAmp, Brain Products, 250 Hz low-pass analogue hardware filter, 10 s time constant, 5 kHz sampling rate, reference electrode: FCz) that were placed on the subject table behind the head coil inside the bore. Data were analysed using Brain Vision Recorder software (Brain Products). The clocks of the EEG amplifiers and MR scanners were synchronized and MR-Volume triggers were acquired for subsequent gradient artifact correction. For the VEP and alpha paradigm the sampling resolution was set to 0.5 μV, resulting in a dynamic range of +/-16.384 mV, to allowed for adequate measurement of the gradient and RF related artifacts related to the ongoing fMRI measurement. For the EEG recordings during the gamma paradigm, the sampling resolution was set to 0.1 μV, resulting in a dynamic range of +/-3.28 mV.

2.7. (f)MRI analysis

The acquired data were converted to NIfTI format (dcm2nii, Chris Rorden, Columbia, SC, USA). The anatomical as well as the mean EPI data shown here were bias field corrected using FSL 5.0.5 (FAST, FMRIB's Software Library (FSL), Oxford, UK. www.fmrib.ox.ac.uk/fsl).

In order to obtain functional maps for the VEP paradigm, the data of the four subjects who performed this paradigm in Essen were analyzed using a general linear model (GLM) as implemented in FSL 5.0.5 (FEAT 6.0). Before the GLM was computed, the data were corrected for motion (MCFLIRT). Brain extraction (BET), high-pass filtering (100 s) and smoothing (5 mm) were applied. Standard FSL hemodynamic response function (HRF) convolved stick functions at stimuli onsets were used as regressors, and movement parameters from the MR volume realignment were used as confound regressors. Subsequent to the individual GLMs, a mixed effect group GLM was performed.

For the alpha and gamma paradigms, only the EEG data were analyzed in this study.

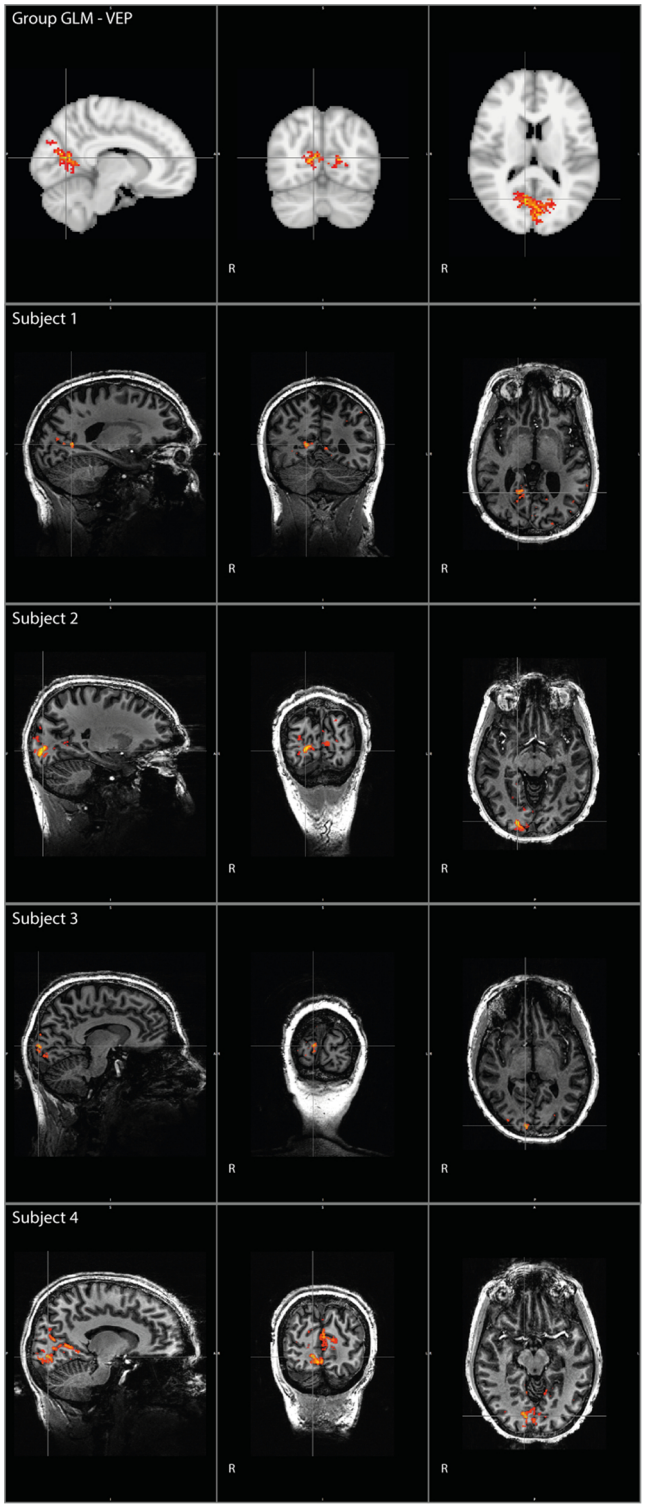

Fig. 5. Group and individual GLM results of the VEP paradigm. Slices are selected to show the most significant voxel.

2.8. EEG analysis

2.8.1. Preprocessing

MR-related gradient artifacts were removed from the EEG data using average subtraction (Allen et al., 2000) as implemented in Analyzer 2 (Brain Products, Gilching, Germany). Subsequently, using Analyzer 2, the data were down-sampled to 250 Hz and filtered (Butterworth Zero Phase Filters: Low Cutoff: 0.5 Hz, 48 dB/oct, High Cutoff: 50 Hz, 48 dB/oct; Notch Filter: 50 Hz), pulse artifacts were labeled and the data were exported to Matlab (Natick, Massachusetts, The MathWorks Inc.). Based on the pulse artifact labels, cardiac-related artifacts were removed, using the optimal basis set (OBS) approach with 4 principal components (PC) as FMRIB plug-in for EEGLAB (Delorme and Makeig, 2004; Niazy et al., 2005).

2.8.2. VEP paradigm

The VEP data were analyzed in Fieldtrip (Oostenveld et al., 2011). After band-bass filtering (0.5 – 20 Hz) the EEG data were segmented into trials starting 0.4 s before and ending 0.8 s after stimulus onset. Temporal independent component analysis (ICA) (Hyvarinen, 1999) was applied to the concatenated trials, and components representing eye-blinks, eye-movements and other artifacts such as electrode and cable movements were removed (9–12 components per subject). After back projecting the remaining components, individual trials with residual artifacts were rejected based on a semi-automatic approach implemented in Fieldtrip. For the remaining trials and for each channel separately, the average over trials was computed, and subsequently baseline corrected by subtracting the average potential in the 400 ms prior to stimulus onset. Before computing the grand average evoked potential over subjects, the individual ERPs for all channels were normalized by dividing all values by the root-mean-square potential over all channels and time-points.

2.8.3. Alpha paradigm

In order to correct eye-blink related artifacts a temporal (infomax) ICA-based (Bell and Sejnowski, 1995) approach implemented in Vision Analyzer 2 (Brainpoducts) was applied on the entire time-series. Up to two eye-blink related components were manually selected based on their time line and potential distribution and removed from the data. The data were further processed in Fieldtrip (Oostenveld et al., 2011). First, the data were re-referenced to the common average and segmented, and the 20 s eyes open and eyes-closed segments were subdivided into 10 non-overlapping epochs of two seconds. Subsequently, the first epoch of 2 s after the eyes were opened or closed and epochs with artifacts (based on visual inspection) were discarded. Power was calculated for 0.5 – 25 Hz in steps of 0.5 Hz based on a multi-taper approach (Mitra and Pesaran, 1999) with +/- 1.5 Hz smoothing in the frequency domain. Average power over segments were computed for the eyes open and closed conditions. For each channel separately, relative power change was calculated as the log-transformed ratio of the average power for the eyes-open and eyes-closed conditions. The grand average power effect was computed by calculating for each channel separately the mean over subjects of this relative power change.

2.8.4. Gamma paradigm

The analysis of the EEG data for the gamma task is described in detail in Scheeringa et al. (2016). In short, we used a denoising strategy approach based on the work by Debener et al. (2006; 2005) that uses temporal ICA (Hyvarinen, 1999) to obtain narrow band gamma band responses (Scheeringa et al., 2011a, 2016). In this approach, we identify one or more components that showed a sustained increase in power compared to baseline in a narrow frequency band. The estimation of the ICA unmixing weight is based on the gamma band (40 – 90 Hz) filtered data. Since we intend to investigate whether we can observe such a gamma band increase but are not interested in the attention effect, the results presented here are collapsed over the attention 'on and 'off' conditions without a speed change. The time-frequency analysis is based on a multitaper approach using sliding temporal window of 400 ms and +/- 10 Hz frequency smoothing, resulting in 7 tapers. These analyses were carried out in Fieldtrip (Oostenveld et al., 2011).

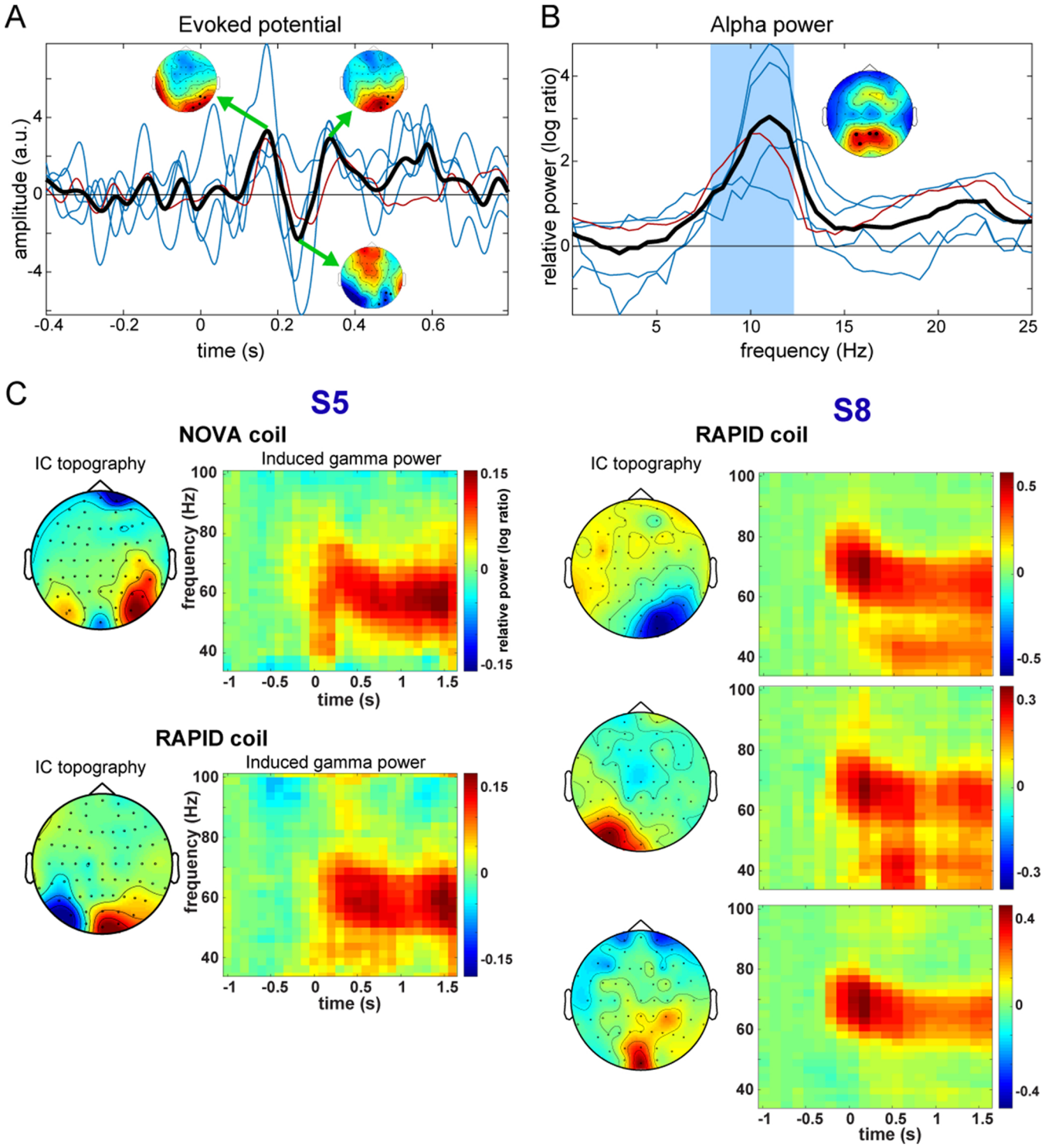

Fig. 6. EEG results. Panel A depicts the individual (blue and red) and grand average (black) visual evoked potential averaged over the indicated channels. The individual ERPs were normalized by dividing the ERP in all channels by the root-mean square over all channels and all depicted time points. Panel B depicts the relative power change for eyes closed versus eyes open in a similar way. The relative power change was computed as the log of the ratio between eyes closed and eyes open EEG power. The classical alpha band (8 – 12 Hz) is indicated by the blue shaded area. For both panels A and B the red line indicates the subject measured in the Phillips scanner in Utrecht, the blue lines depict the individual responses measured in the Siemens scanner. Panel C Depicts the time frequency analysis of the individual independent components that showed the expected narrow band gamma response and their associated topographies for the two subjects for which this response was observed. Note that the polarity of the independent components is arbitrary. The separate recordings inside the NOVA and RAPID coils are indicated. The power values in the time-frequency representation are computed as the log ratio over the power values 200 – 300 ms before trial onset.

3. Results

3.1. Adaptation of the EEG cap

Fig. 1 **B)** and **C) demonstrate how** the cable and connectors of the adapted 64 channel EEG cap (Fig. 1A**)**) pass through the opening at the back of the opened NOVA head coil. Once the coil is closed, the flat part of the cable passes through the gap between the upper and lower parts of the coil, allowing the EEG cap to function within the coil. Before and after scanning sessions the temperature of the subjects was measured, and no noticeable change was recorded for subjects scanned with the adapted MRI compatible EEG cap.

3.2. Quality of (f)MRI data

Using the NOVA head coil for combined EEG-fMRI significantly improves the MRI data quality compared to the recommended setup. Fig. 3 shows a comparison of T1 images recorded with the recommended setup using the RAPID coil from one subject with a common 64 channel EEG cap (Fig. 3, right bottom) and the new setup including the NOVA head coil and the new 64 channel EEG cap at three different institutes (Fig. 3, all other anatomical scans). The recommended setup leads to severe signal drop out at the upper part of the head, and a lower quality anatomical scan in general. In contrast, using the NOVA head coil together with the new 64 channel EEG cap results in almost unaffected MR image quality of the T1 images as compared to T1 images acquired without the EEG cap. This improvement in T1 image quality was reproducible across subjects, sites and systems.

Similar as for the anatomical scans, Fig. 4 depicts the mean EPI images. For subject 5 we show the mean EPI image measured with both the NOVA and RAPID coils. Note the reduced coverage for the EPIs measured with the RAPID coil, for which resolution and image acquisition time were kept the same as for the NOVA coil. In general the adapted cap seems to cause some signal loss in both RAPID and NOVA coils, but this can be adjusted for adequately by a relatively straightforward bias field correction as implemented in FSL FAST (Zhang et al., 2001), as is depicted in this figure. Fig. 5 depicts the results of the group and individual GLMs for the VEP paradigm. Slices are selected to show the most significant voxel. The group results show the expected relation of the visual cortex to the visual lower left checkerboard stimuli, with a maximum cluster on the right side. All subjects consistently showed the largest activation clusters in the right hemisphere of visual cortex contralateral to the side of stimulation.

These results demonstrate that it is feasible to measure brain anatomy and BOLD activity with the 32 channel NOVA coil while wearing the modified EEG cap.

3.3. Quality of the EEG data

The results of the EEG analysis of the three distinct paradigms show that the known responses of all three paradigms could be reproduced in a 7 T environment and measured with the modified EEG cap (see Fig. 6). The observed effects correspond with those earlier observed at 7 T (Jorge et al., 2015; Vasios et al., 2006) or lower field strengths (Feige et al., 2005; Scheeringa et al., 2011a, b) in the MRI environment and those recorded with EEG or MEG (Hoogenboom et al., 2006; Koch et al., 2009; Muthukumaraswamy and Singh, 2008). Fig. 6A depicts the results of the VEP paradigm, showing the grand average across the 5 subjects and the individual VEPs. The grand average, and to a lesser extent also the individual ERPs, show prominent P1, N1 and P2 components, of which the P1 is strongest over right posterior occipital cortex, in line with left hemifield stimulation in this paradigm.

In Fig. 6B the relative change in power for the eyes-closed versus eyes-open condition is shown. For all subjects, power in the alpha band was higher during the eyes-closed compared to the eyes-open condition, with a peak effect located between 9.5 and 12.5 Hz.

Fig. 6C depicts the gamma band responses to the visual attention task for subjects 5 an 8. For both subjects the topographies and time-frequency representation of power for independent components with the expected gamma band response are shown. For subject 5 this is shown for data recorded both in the RAPID and NOVA coils. For subject 8 the data were recorded inside the RAPID coil. The data here demonstrated that the high EEG frequency range can in principle be recorded in the 7 T environment using the new modified cap inside both NOVA and RAPID coils. For the other subjects who performed this task we were however not able to identify the expected narrow band gamma response.

Together, the ability to measure these well documented EEG responses indicate it is feasible to measure EEG with the adapted cap simultaneously with fMRI in the 7 T MRI environment.

4. Discussion

In this study we demonstrate how we adapted an MRI compatible EEG cap that allows for the measurement of good quality EEG and (f) MRI inside the closed 32 channel NOVA-coil. We demonstrate this by presenting anatomical MRI data, and simultaneously recorded EEG and fMRI data. We compared the quality of both functional and anatomical images and some of the EEG responses with similar measurements obtained with the recommended EEG set-up using the RAPID-coil. Good quality images without substantial signal distortions recorded with the NOVA-coil were obtained for both functional and anatomical scans for both Siemens and Philips 7 T systems. Adverse effects of the electrodes and wires on B0 homogeneity were confined to regions close to the electrodes, and the new cabling configuration ameliorated the effect on B1-homogeneity so that the proposed system allows normal imaging procedures.

In the EEG data we observed that the alpha band modulation by the eyes-open/eyes-closed paradigm and the visual evoked responses in response to the checkerboard wedge is in line with the literature (Berger, 1929; Luck et al., 2000), and comparable in quality to previous measurements in a 7 T environment (Jorge et al., 2015; Vasios et al., 2006) and lower field strengths (Becker et al., 2005; Ostwald et al., 2010; Porcaro et al., 2010). In addition to these two features, we demonstrated that it is possible to measure gamma band synchronization during a visual attention task that is similar to that observed in animal LFP recording (Fries et al., 2008), human MEG/EEG recordings (Hoogenboom et al., 2006; Muthukumaraswamy and Singh, 2008) and EEG recorded in a 3 T MRI scanner (Scheeringa et al., 2016, 2011b). This gamma component was however only observed in only two of the six subjects. This indicates that the 7 T environment might be more problematic for the measurement of high frequency gamma band activity than the 3 T environment, where we could observe this effect in the vast majority of subjects (Scheeringa et al., 2016, 2011b). This can possibly be counteracted by taking even greater care of minimizing subject and cable movement and pre-selecting subjects with a strong gamma-band response. A factor that might have affected the ability to identify gamma related ICA components is that in 3 of the 6 subjects only one block of the gamma task was performed. For the two subjects for which a gamma band response was observed three blocks were measured. The results, however, indicate that it is possible to measure gamma band activity with both the recommended setup in the RAPID coil as well as with our adapted cap in the NOVA coil. Overall, these results indicate the feasibility to record EEG simultaneously with (high resolution) fMRI in the 7 T MRI environment for a representative set of EEG experiments, and without major compromises to the (f)MRI acquisition in terms of signal drop-out, spatial coverage and resolution.

For functional imaging studies one of the most important advantages of high field fMRI is that it allows for the measurement of neuronal activity at high spatial resolution with a better SNR than lower field (1.5/3 T) and a higher acquisition efficiency which may be

manifest as either larger coverage, higher spatial or temporal resolution, or a combination thereof. The higher resolution makes it possible to study layer specific neuronal activity in humans non-invasively. Activity in different cortical layers is related to frequency specific changes in electrophysiology (Bastos et al., 2015; Bollimunta et al., 2008, 2011; Buffalo et al., 2011; Maier et al., 2011) that can be recorded simultaneously with EEG (Scheeringa et al., 2011a, 2016). At 3 T, these oscillations recorded simultaneously with EEG show laminar specific correlations with the BOLD signal (Scheeringa et al., 2016). Furthermore (high resolution) fMRI at 7 T makes it possible to scan relatively small sub-cortical nuclei in more detail and higher SNR than at lower field strengths (Balchandani and Naidich, 2015). Electrophysiological recordings have been directly related to activity in subcortical structures (Lopes da Silva et al., 1980; Saalmann et al., 2012). Combined EEG and fMRI at 7 T would therefore allow the study of the relationship between BOLD activity in subcortical structures and scalp level EEG features at finer detail than at lower field strengths.

Several previous simultaneous EEG-fMRI studies have focused on the association between spontaneous resting state fluctuations in frequency specific EEG power and fMRI/BOLD activity across the entire brain (de Munck et al., 2007d; Goncalves et al., 2006; Laufs et al., 2006, 2003; Mantini et al., 2007; Sadaghiani et al., 2010; Scheeringa et al., 2008). Often specific BOLD-defined resting state networks were found to correlate with these EEG power measures (Mantini et al., 2007; Sadaghiani et al., 2010; Scheeringa et al., 2008). MEG resting state studies have suggested that these networks can also be found in source level alpha/beta fluctuations (Brookes et al., 2011a, b). In animal research alpha and beta oscillations are often observed to originate from deep layers (Bollimunta et al., 2008, 2011; Buffalo et al., 2011; Maier et al., 2010, 2011; Spaak et al., 2012; van Kerkoerle et al., 2014v) and have also been linked to specific subcortical nuclei (Lopes da Silva et al., 1980; Saalmann et al., 2012). By measuring EEG simultaneously with high resolution fMRI at 7 T it will be possible to investigate which cortical layers and subcortical nuclei relate to power changes of interest and to investigate this for the entire brain at the same time. In a similar way, combining whole brain high-resolution fMRI at 7 T with EEG can be a viable technique to investigate the laminar specific correlates of event related potentials and task related changes in EEG power across the cortex, while simultaneously investigating whether they relate to involvement of sub-cortical brain regions. This was not possible for previous studies that measured EEG and fMRI simultaneously in a task context at lower field strengths. This represents an important advance since the subcortical regions are thought to play a pivotal role in frequency and laminar specific neural processes (Saalmann and Kastner, 2011; Saalmann et al., 2012).

The current study is a technical report that documents the steps we undertook to obtain good quality recordings of both (f)MRI and EEG during simultaneous measurements at 7 T. The studies that report on simultaneous EEG and fMRI at 7 T have to date also been of a technical nature and address either (f)MRI acquisition, subject safety and EEG data quality and EEG data analysis approaches (Abbasi et al., 2015; Brookes et al., 2009; Jorge et al., 2015; Mullinger et al., 2008a, b; Poulsen et al., 2017; Vasios et al., 2006). In general these studies concluded that, although the 7 T environment causes larger distortions in MR images and an enlarged cardiobalistic artifact in the EEG, simultaneous EEG and fMRI at 7 T can be safely measured(Jorge et al., 2015; Mullinger et al., 2008a, b; Poulsen et al., 2017). To the best of our knowledge, no studies have hitherto reported combined EEG and fMRI at 7 T in a task, resting state or clinical setting. The added benefits of combining EEG and fMRI at 7 T are therefore initially best explored with paradigms and experimental conditions that have previously yielded reliable results for combined EEG & fMRI at lower field strengths.

The MR-acquisition protocols that we used are representative for fMRI investigations at 7 T without necessarily being at the highest spatial or temporal resolution attainable. There is however, no reason to assume that the results obtained would differ qualitatively for higher resolution acquisitions.

In conclusion, the adaptations we made to the 64-channel EEG cap allowed us to measure EEG simultaneously with fMRI recorded with a 32 channel NOVA coil on both Siemens and Phillips 7 T MRI systems. The results indicate improved (f)MRI data quality compared to a recommended set-up with an open ended bird-cage RAPID coil, while retaining good quality EEG recordings that allow for the measurements of well-known EEG features. These recordings indicate that it is in principle feasible to combine high resolution (laminar level) fMRI with simultaneous recorded EEG.

CRediT authorship contribution statement

Matthias C. Meyer: Conceptualization, Data curation, Formal analysis, Investigation, Methodology, Resources, Software, Visualization, Writing - original draft. **René Scheeringa:** Data curation, Formal analysis, Funding acquisition, Investigation, Methodology, Resources, Software, Visualization, Writing - original draft, Writing - review & editing. **Andrew G. Webb:** Conceptualization, Funding acquisition, Resources. **Natalia Petridou:** Conceptualization, Funding acquisition, Resources. **Oliver Kraff:** Data curation, Investigation, Resources. **David G. Norris:** Conceptualization, Resources, Supervision, Visualization, Writing - review & editing.

Acknowledgements

This work was supported by a grant from the Netherlands Organization for Scientific Research176.010.2005.030 (MCM, AGW, NP, DGN) and the Netherlands Organization for Scientific Research by the Veni scheme451-12-021 (to R.S.).

The funder had no role in study design, data collection and analysis, decision to publish, or preparation of the manuscript.

References

Abbasi, O., Dammers, J., Arrubla, J., Warbrick, T., Butz, M., Neuner, I., Shah, N.J., 2015. Time-frequency analysis of resting state and evoked EEG data recorded at higher magnetic fields up to 9.4 T. J. Neurosci. Methods 255, 1–11.

Allen, P.J., Josephs, O., Turner, R., 2000. A method for removing imaging artifact from continuous EEG recorded during functional MRI. Neuroimage 12, 230–239.

Balchandani, P., Naidich, T.P., 2015. Ultra-high-Field MR neuroimaging. AJNR Am. J. Neuroradiol. 36, 1204–1215.

Bastos, A.M., Vezoli, J., Bosman, C.A., Schoffelen, J.M., Oostenveld, R., Dowdall, J.R., De Weerd, P., Kennedy, H., Fries, P., 2015. Visual areas exert feedforward and feedback influences through distinct frequency channels. Neuron 85, 390–401.

Becker, R., Ritter, P., Moosmann, M., Villringer, A., 2005. Visual evoked potentials recovered from fMRI scan periods. Hum. Brain Mapp. 26, 221–230.

Bell, A., Sejnowski, T., 1995. An information-maximization approach to blind separation and blind deconvolution. Neural Comput. 7, 1129–1159.

Berger, H., 1929. Über das elektrenkephalogramm des menschen. Archiv für Psychiatrie und Nervenkrankheiten 87, 527–570.

Bollimunta, A., Chen, Y., Schroeder, C.E., Ding, M., 2008. Neuronal mechanisms of cortical alpha oscillations in awake-behaving macaques. J. Neurosci. 28, 9976–9988.

Bollimunta, A., Mo, J., Schroeder, C.E., Ding, M., 2011. Neuronal mechanisms and attentional modulation of corticothalamic alpha oscillations. J. Neurosci. 31, 4935–4943.

Brookes, M.J., Hale, J.R., Zumer, J.M., Stevenson, C.M., Francis, S.T., Barnes, G.R., Owen, J.P., Morris, P.G., Nagarajan, S.S., 2011a. Measuring functional connectivity using MEG: methodology and comparison with fcMRI. NeuroImage 56, 1082–1104.

Brookes, M.J., Vrba, J., Mullinger, K.J., Geirsdottir, G.B., Yan, W.X., Stevenson, C.M., Bowtell, R., Morris, P.G., 2009. Source localisation in concurrent EEG/fMRI: applications at 7T. NeuroImage 45, 440–452.

Brookes, M.J., Woolrich, M., Luckhoo, H., Price, D., Hale, J.R., Stephenson, M.C., Barnes, G.R., Smith, S.M., Morris, P.G., 2011b. Investigating the electrophysiological basis of resting state networks using magnetoencephalography. Proc. Natl. Acad. Sci. U. S. A. 108, 16783–16788.

Buffalo, E.A., Fries, P., Landman, R., Buschman, T.J., Desimone, R., 2011. Laminar differences in gamma and alpha coherence in the ventral stream. Proc. Natl. Acad. Sci. U. S. A. 108, 11262–11267.

de Munck, J.C., Goncalves, S.I., Huijboom, L., Kuijer, J.P., Pouwels, P.J., Heethaar, R.M., Lopes da Silva, F.H., 2007d. The hemodynamic response of the alpha rhythm: an EEG/fMRI study. NeuroImage 35, 1142–1151.

Debener, S., Ullsperger, M., Siegel, M., Engel, A.K., 2006. Single-trial EEG-fMRI reveals the dynamics of cognitive function. Trends. Cogn. Sci. 10, 558–563.

Debener, S., Ullsperger, M., Siegel, M., Fiehler, K., von Cramon, D.Y., Engel, A.K., 2005. Trial-by-trial coupling of concurrent electroencephalogram and functional magnetic resonance imaging identifies the dynamics of performance monitoring. J. Neurosci. 25, 11730–11737.

Delorme, A., Makeig, S., 2004. EEGLAB: an open source toolbox for analysis of single-trial EEG dynamics including independent component analysis. J. Neurosci. Methods 134, 9–21.

Eichele, T., Specht, K., Moosmann, M., Jongsma, M.L.A., Quiroga, R.Q., Nordby, H., Hugdahl, K., 2005. Assessing the spatiotemporal evolution of neuronal activation with single-trial event-related potentials and functional MRI. Proc. Natl. Acad. Sci. U. S. A. 102, 17798–17803.

Feige, B., Scheffler, K., Esposito, F., Di Salle, F., Hennig, J., Seifritz, E., 2005. Cortical and subcortical correlates of electroencephalographic alpha rhythm modulation. J. Neurophysiol. 93, 2864–2872.

Fries, P., Scheeringa, R., Oostenveld, R., 2008. Finding gamma. Neuron 58, 303–305.

Goncalves, S.I., de Munck, J.C., Pouwels, P.J., Schoonhoven, R., Kuijer, J.P., Maurits, N.M., Hoogduin, J.M., Van Someren, E.J., Heethaar, R.M., 2006. Lopes da Silva FH. Correlating the alpha rhythm to BOLD using simultaneous EEG/fMRI: inter-subject variability. NeuroImage 30, 203–213.

Hoogenboom, N., Schoffelen, J.M., Oostenveld, R., Parkes, L.M., Fries, P., 2006. Localizing human visual gamma-band activity in frequency, time and space. NeuroImage 29, 764–773.

Hyvarinen, A., 1999. Fast and robust fixed-point algorithms for independent component analysis. IEEE Trans. Neural Netw. 10, 626–634.

Jorge, J., Grouiller, F., Ipek, O., Stoermer, R., Michel, C.M., Figueiredo, P., van der Zwaag, W., Gruetter, R., 2015. Simultaneous EEG-fMRI at ultra-high field: artifact prevention and safety assessment. NeuroImage 105, 132–144.

Koch, S.P., Werner, P., Steinbrink, J., Fries, P., Obrig, H., 2009. Stimulus-induced and state-dependent sustained gamma activity is tightly coupled to the hemodynamic response in humans. J. Neurosci. 29, 13962–13970.

Laufs, H., Holt, J.L., Elfont, R., Krams, M., Paul, J.S., Krakow, K., Kleinschmidt, A., 2006. Where the BOLD signal goes when alpha EEG leaves. NeuroImage 31, 1408–1418.

Laufs, H., Kleinschmidt, A., Beyerle, A., Eger, E., Salek-Haddadi, A., Preibisch, C., Krakow, K., 2003. EEG-correlated fMRI of human alpha activity. NeuroImage 19, 1463–1476.

Lopes da Silva, F.H., Vos, J.E., Mooibroek, J., Van Rotterdam, A., 1980. Relative contributions of intracortical and thalamo-cortical processes in the generation of alpha rhythms, revealed by partial coherence analysis. Electroencephalogr. Clin. Neurophysiol. 50, 449–456.

Luck, S.J., Woodman, G.F., Vogel, E.K., 2000. Event-related potential studies of attention. Trends Cogn. Sci. 4, 432–440.

Maier, A., Adams, G.K., Aura, C., Leopold, D.A., 2010. Distinct superficial and deep laminar domains of activity in the visual cortex during rest and stimulation. Front. Syst. Neurosci. 4.

Maier, A., Aura, C.J., Leopold, D.A., 2011. Infragranular sources of sustained local field potential responses in macaque primary visual cortex. J. Neurosci. 31, 1971–1980.

Mantini, D., Perrucci, M.G., Del Gratta, C., Romani, G.L., Corbetta, M., 2007. Electrophysiological signatures of resting state networks in the human brain. Proc. Natl. Acad. Sci. U. S. A. 104, 13170–13175.

Mitra, P.P., Pesaran, B., 1999. Analysis of dynamic brain imaging data. Biophys. J. 76, 691–708.

Moosmann, M., Schonfelder, V.H., Specht, K., Scheeringa, R., Nordby, H., Hugdahl, K., 2009. Realignment parameter-informed artefact correction for simultaneous EEG-fMRI recordings. NeuroImage 45, 1144–1150.

Mullinger, K., Brookes, M., Stevenson, C., Morgan, P., Bowtell, R., 2008a. Exploring the feasibility of simultaneous electroencephalography/functional magnetic resonance imaging at 7 T. Magn. Reson. Imaging 26, 968–977.

Mullinger, K., Debener, S., Coxon, R., Bowtell, R., 2008b. Effects of simultaneous EEG recording on MRI data quality at 1.5, 3 and 7 tesla. Int. J. Psychophysiol. 67, 178–188.

Muthukumaraswamy, S.D., Singh, K.D., 2008. Spatiotemporal frequency tuning of BOLD and gamma band MEG responses compared in primary visual cortex. NeuroImage 40, 1552–1560.

Nehrke, K., Bornert, P., 2012. DREAM–a novel approach for robust, ultrafast, multislice B(1) mapping. Magn. Reson. Med. 68, 1517–1526.

Neuner, I., Warbrick, T., Arrubla, J., Felder, J., Celik, A., Reske, M., Boers, F., Shah, N.J., 2013. EEG acquisition in ultra-high static magnetic fields up to 9.4 T. NeuroImage 68, 214–220.

Niazy, R.K., Beckmann, C.F., Iannetti, G.D., Brady, J.M., Smith, S.M., 2005. Removal of FMRI environment artifacts from EEG data using optimal basis sets. NeuroImage 28, 720–737.

Oostenveld, R., Fries, P., Maris, E., Schoffelen, J.M., 2011. FieldTrip: open source software for advanced analysis of MEG, EEG, and invasive electrophysiological data. Comput. Intell. Neurosci. 2011, 156869.

Ostwald, D., Porcaro, C., Bagshaw, A.P., 2010. An information theoretic approach to EEG-fMRI integration of visually evoked responses. NeuroImage 49, 498–516.

Porcaro, C., Ostwald, D., Bagshaw, A.P., 2010. Functional source separation improves the quality of single trial visual evoked potentials recorded during concurrent EEG-fMRI. NeuroImage 50, 112–123.

Poulsen, C., Wakeman, D.G., Atefi, S.R., Luu, P., Konyn, A., Bonmassar, G., 2017. Polymer thick film technology for improved simultaneous dEEG/MRI recording: safety and MRI data quality. Magn. Reson. Med. 77, 895–903.

Saalmann, Y.B., Kastner, S., 2011. Cognitive and perceptual functions of the visual thalamus. Neuron 71, 209–223.

Saalmann, Y.B., Pinsk, M.A., Wang, L., Li, X., Kastner, S., 2012. The pulvinar regulates information transmission between cortical areas based on attention demands. Science 337, 753–756.

Sadaghiani, S., Scheeringa, R., Lehongre, K., Morillon, B., Giraud, A.L., Kleinschmidt, A., 2010. Intrinsic connectivity networks, alpha oscillations, and tonic alertness: a simultaneous electroencephalography/functional magnetic resonance imaging study. J. Neurosci. 30, 10243–10250.

Scheeringa, R., Bastiaansen, M.C., Petersson, K.M., Oostenveld, R., Norris, D.G., Hagoort, P., 2008. Frontal theta EEG activity correlates negatively with the default mode network in resting state. Int. J. Psychophysiol. 67, 242–251.

Scheeringa, R., Fries, P., Petersson, K.M., Oostenveld, R., Grothe, I., Norris, D.G., Hagoort, P., Bastiaansen, M.C., 2011a. Neuronal dynamics underlying high- and low-frequency EEG oscillations contribute independently to the human BOLD signal. Neuron 69, 572–583.

Scheeringa, R., Koopmans, P.J., van Mourik, T., Jensen, O., Norris, D.G., 2016. The relationship between oscillatory EEG activity and the laminar-specific BOLD signal. Proc. Natl. Acad. Sci. U. S. A. 113, 6761–6766.

Scheeringa, R., Mazaheri, A., Bojak, I., Norris, D.G., Kleinschmidt, A., 2011b. Modulation of visually evoked cortical FMRI responses by phase of ongoing occipital alpha oscillations. J. Neurosci. 31, 3813–3820.

Scheeringa, R., Petersson, K.M., Kleinschmidt, A., Jensen, O., Bastiaansen, M.C., 2012. EEG alpha power modulation of fMRI resting-state connectivity. Brain Connect. 2, 254–264.

Scheeringa, R., Petersson, K.M., Oostenveld, R., Norris, D.G., Hagoort, P., Bastiaansen, M.C., 2009. Trial-by-trial coupling between EEG and BOLD identifies networks related to alpha and theta EEG power increases during working memory maintenance. NeuroImage 44, 1224–1238.

Spaak, E., Bonnefond, M., Maier, A., Leopold, D.A., Jensen, O., 2012. Layer-specific entrainment of gamma-band neural activity by the alpha rhythm in monkey visual cortex. Curr. Biol. 22, 2313–2318.

van Kerkoerle, T., Self, M.W., Dagnino, B., Gariel-Mathis, M.A., Poort, J., van der Togt, C., Roelfsema, P.R., 2014v. Alpha and gamma oscillations characterize feedback and feedforward processing in monkey visual cortex. Proc. Natl. Acad. Sci. U. S. A. 111, 14332–14341.

Vasios, C.E., Angelone, L.M., Purdon, P.L., Ahveninen, J., Belliveau, J.W., Bonmassar, G., 2006. EEG/(f)MRI measurements at 7 Tesla using a new EEG cap ("InkCap"). NeuroImage 33, 1082–1092.

Vitali, P., Di Perri, C., Vaudano, A.E., Meletti, S., Villani, F., 2015. Integration of multimodal neuroimaging methods: a rationale for clinical applications of simultaneous EEG-fMRI. Funct. Neurol. 30, 9–20.

Zhang, Y., Brady, M., Smith, S., 2001. Segmentation of brain MR images through a hidden Markov random field model and the expectation-maximization algorithm. IEEE Trans. Med. Imaging 20, 45–57.